Constraining the quintessence equation of state with SnIa data and CMB peaks

Pier Stefano Corasaniti* and Edmund J. Copeland†
Centre for Theoretical Physics, University of Sussex, Brighton, BN1 9QJ, United Kingdom
(Received 19 July 2001; revised manuscript received 3 October 2001; published 22 January 2002)

Quintessence has been introduced as an alternative to the cosmological constant scenario to account for the current acceleration of the universe. This new dark energy component allows values of the equation of state parameter $w_Q^0 \geqslant -1$ and in principle measurements of cosmological distances to type Ia supernovae can be used to distinguish between these two types of models. Assuming a flat universe, we use the supernovae data and measurements of the position of the acoustic peaks in the cosmic microwave background spectra to constrain a rather general class of quintessence potentials, including inverse power law models and recently proposed supergravity inspired potentials. In particular we use a likelihood analysis, marginalizing over the dark energy density Ω_Q, the physical baryon density $\Omega_b h^2$ and the scalar spectral index n, to constrain the slopes of our quintessence potential. Considering only the first Doppler peak the best fit in our range of models gives $w_Q^0 \sim -0.8$. However, including the SnIa data and the three peaks, we find an upper limit on the present value of the equation of state parameter, $-1 \leqslant w_Q^0 \leqslant -0.93$ at 2σ, a result that appears to rule out a class of recently proposed potentials.

DOI: 10.1103/PhysRevD.65.043004 PACS number(s): 98.70.Vc

I. INTRODUCTION

Observations of distant type Ia supernovae [1,2] and small angular scale anisotropies in the cosmic microwave background (CMB) [3–6] suggest that the universe is dominated by a large amount of dark energy with a negative equation of state parameter w. One obvious explanation would be the presence for all time of a cosmological constant with $w=-1$, although there is no satisfactory reason known why it should be so close to the critical energy density (for a general review see [7]). An alternative proposal introduces a new type of matter and is called ''quintessence'' [8]. Assuming that some unknown mechanism cancels the true cosmological constant, this dark energy is associated with a light scalar field Q evolving in a potential $V(Q)$. The equation of state parameter of the Q component is given by

$$w_Q = \frac{\frac{\dot{Q}^2}{2} - V(Q)}{\frac{\dot{Q}^2}{2} + V(Q)} \tag{1}$$

and it is a function of time. According to the form of $V(Q)$ the present value of w_Q is in the range $w_Q^0 \geqslant -1$. The temporal dependence of w_Q implies that high redshift observations could in principle distinguish between the cold dark matter model with a cosmological constant (Λ CDM) and quintessence cold dark matter model (QCDM) [10–14]. Moreover, a number of authors have recently pointed out that the position of the CMB peaks could provide an efficient way to constrain quintessence models [15–17].

In this paper we use the supernovae sample of Perlmutter *et al.* [1] and the recent measurements of the location of the CMB peaks [18] to determine new limits on the quintessence equation of state. Our study is similar in approach to an earlier analysis by Efstathiou [19]. We consider a general class of potentials parametrized in such a way that we can control their shape, and apply a likelihood analysis to find the confidence regions for the parameters of the potential and the best value for the fractional quintessence energy density Ω_Q. The constraints which emerge are different if we analyze the data separately. In particular the position of the first Doppler peak prefers a quintessence model with $w_Q^0 \sim -0.8$ for the prior $\Omega_Q = 0.7$ in agreement with Baccigaluppi *et al.* [20], while the analysis of all the CMB peaks and SnIa gives an upper value for the equation of state, $w_Q^0 \leqslant -0.93$ at 2σ for these class of models. This limit is stronger than those previously obtained [21–23], $w_Q^0 \leqslant -0.6$ at 2σ, simply because we are making use of the new improved CMB data. An obvious consequence of this result is that in these class of models, for them to succeed the scalar field dynamics has to produce effects similar to pure vacuum energy and in this case it is unlikely that quintessence can be distinguished from a cosmological constant (see also [9]).

II. QUINTESSENCE EQUATION OF STATE

The scalar field dynamics is described by the Klein-Gordon equation

$$\ddot{Q} + 3H\dot{Q} + \frac{dV}{dQ} = 0, \tag{2}$$

with

$$H^2 = \frac{8\pi G}{3}\left[\rho_m + \rho_r + \frac{\dot{Q}^2}{2} + V(Q)\right], \tag{3}$$

where ρ_m and ρ_r are the matter and radiation energy densities respectively. It is well known that for a wide class of potentials, Eq. (2) possesses attractor solutions [24]. In this

*Email address: pierc@pact.cpes.susx.ac.uk
†Email address: e.j.copeland@sussex.ac.uk

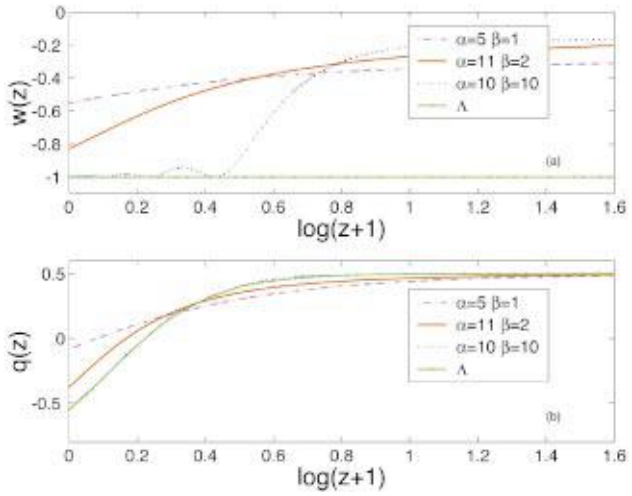

FIG. 1. (Color) In (a) the evolution of w_Q against the redshift is plotted for different values of α and β. In (b) the behavior of the deceleration parameter, q, is plotted against the redshift. The acceleration starts ($q<0$) earlier for models with an equation of state close to that of a true cosmological constant.

regime the kinetic energy of the field is subdominant allowing w_Q to become negative. The present value of w_Q^0 depends on the slope of the potential in the region reached by the field. Actually if the quintessence field rolls down a very flat region [25] or if it evolves close to a minimum [26–28] the equation of state parameter varies in the range $-1 \leqslant w_Q^0 < -0.8$. On the other hand, models such as the inverse power law potential [29,30] require larger values of w_Q^0. A general potential which can accommodate a large class of scenarios is

$$V(Q) = \frac{M^{4+\alpha}}{Q^\alpha} e^{(1/2)(\kappa Q)^\beta}, \tag{4}$$

where $\kappa = \sqrt{8\pi G}$ and M is fixed in such a way that today $\rho_Q = \rho_c \Omega_Q$, where ρ_c is the critical energy density. For $\beta = 0$ Eq. (4) becomes an inverse power law, while for $\beta = 2$ we have the supergravity (SUGRA) potential proposed by [27]. For $\alpha = 0$, $\beta = 1$ and starting with a large value of Q, the quintessence field evolves in a pure exponential potential [31]. We do not consider this case further since it is possible to have a dark energy dominated universe, but at the expense of fine tuning for the initial conditions of the scalar field. Larger values of β mimic the model studied in [28]. For $\alpha, \beta \neq 0$ the potential has a minimum, the dynamics can be summarized as the following. For small values of β and for a large range of initial conditions, the field does not reach the minimum by the present time and hence $w_Q^0 > -1$. For example, if the quintessence energy density initially dominates over the radiation, the Q field quickly rolls down the inverse power law part of the potential eventually resting in the minimum with $w_Q \sim -1$ after a series of damped oscillations [32]. This behavior however requires fine tuning the initial value of Q to be small. On the other hand, this can be avoided if we consider large values of α and β [Fig. 1(a)]. In these models the fractional energy density of the quintessence field, Ω_Q, is always negligible during both radiation and matter dominated eras. In fact, for small initial values of Q, $V(Q)$ acts like an inverse power law potential, hence as Q enters the scaling regime its energy density is subdominant compared to that of the background component. Therefore nucleosynthesis constraints [33] are always satisfied and there are no physical effects on the evolution of the density perturbations. The main consequence is that for a different value of w_Q^0 the Universe starts to accelerate at a different redshift [Fig. 1(b)].

This implies that different values of α and β lead to a different luminosity distance and angular diameter distance. Consequently by making use of the observed distances we may in principle determine an upper limit on w_Q^0, potentially constraining the allowed shape of the quintessence potential [10].

III. CMB PEAKS

The CMB power spectrum provides information on combinations of the fundamental cosmological quantities. The position of the Doppler peaks depends on the geometry of the Universe through the angular diameter distance, although the amplitude of the peaks are sensitive to many different parameters. The important point for us is that in general the quintessence field can contribute to the shape of the spectrum through both the early integrated Sachs-Wolfe (ISW) effect and the late one [34]. The former is important if the dark energy contribution at the last scattering surface (LSS) is not negligible [35,25] or in non-minimally coupled models [36–38], whereas the late ISW effect is the only effect in models with $\Omega_Q \sim 0$ at LSS [39]. However, as has recently been demonstrated an accurate determination of the position of the Doppler peaks is more sensitive to the actual amount of dark energy [17]. To be more precise, the multipole of the mth peak is $l_m = m l_{sh}$, where l_{sh} is proportional to the angular scale of the sound horizon at LSS. In a flat universe l_{sh} is given by

$$l_{sh} = \frac{\pi}{\overline{c_s}} \left(\frac{\tau_0}{\tau_{ls}} - 1 \right), \tag{5}$$

where $\overline{c_s}$ is the mean sound velocity and τ_0, τ_{ls} are the conformal time today and at last scattering respectively. However, physical effects before recombination can shift the scale of the sound horizon at different multipoles, resulting in a better estimate for the peak positions being given by

$$l_m = l_{sh}(m - \delta l - \delta l_m), \tag{6}$$

where δl is an overall shift [40] and δl_m is the shift of the mth peak. These corrections depend on the amount of baryons $\Omega_b h^2$, on the fractional quintessence energy density at last scattering (Ω_Q^{ls}) and today (Ω_Q^0), as well as on the scalar spectral index n. Recently, analytic formulas, valid over a large range of the cosmological parameters, have been provided to good accuracy for δl and δl_m [41]. Of crucial importance is the observation that the position of the third peak

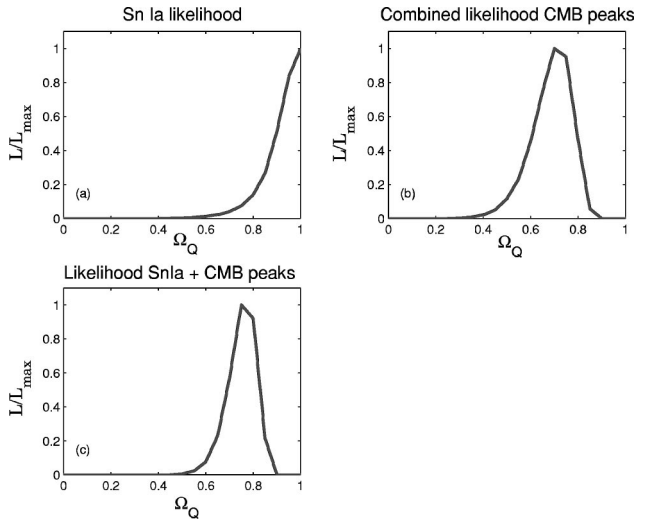

FIG. 2. Fractional quintessence energy density likelihoods, (a) for SnIa, (b) for the combined CMB peaks and (c) for the combined data sets.

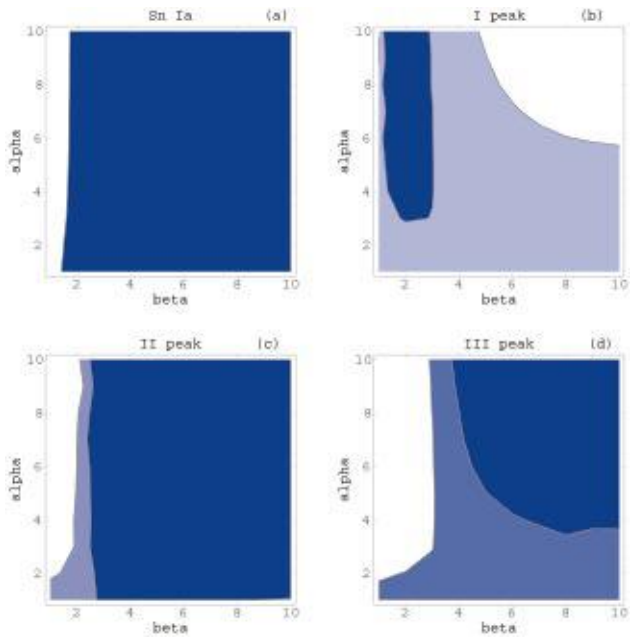

FIG. 3. (Color) Likelihood contour plots for SnIa, I, II and III acoustic peaks. The blue region is the 68% confidence region while the 90% is the light blue one. For the SnIa the white region correspond to 2σ. The position of the third CMB acoustic peak strongly constrains the acceptable parameter space.

appears to remain insensitive to other cosmological quantities, hence we can make use of this fact to test dark energy models [42].

IV. LIKELIHOOD ANALYSIS AND RESULTS

A. Constraints from supernovae

We want to constrain the set of parameters α, β and Ω_Q confined in the range: $\alpha \in (1,10)$, $\beta \in (0,10)$ and $\Omega_Q \in (0,1)$, subject to the assumption of a flat universe. We use the SnIa data fit C of Perlmutter *et al.* [1], that excludes 4 high redshift data points. The magnitude-redshift relation is given by

$$m(z) = 5 \log D_L(z,\alpha,\beta,\Omega_Q) + \mathcal{M}, \tag{7}$$

where $\mathcal{M}$ is the ''Hubble constant free'' absolute magnitude and $D_L(z) = H_0 d_L(z)$ is the free-Hubble constant luminosity distance. In a flat universe,

$$d_L(z) = (\tau_0 - \tau(z))(1+z), \tag{8}$$

where τ_0 is the conformal time today and $\tau(z)$ is the conformal time at the red-shift z of the observed supernova. Both of these quantities are calculated solving numerically Eq. (2) and Eq. (3) for each value of α, β and Ω_Q. In $\mathcal{M}$ we neglect the dependence on a fifth parameter (α in [1]) and assume it to be 0.6, best value in [1]. We then obtain a Gaussian likelihood function $\mathcal{L}^{\mathcal{S}\backslash n}(\alpha,\beta,\otimes_Q)$, by marginalizing over $\mathcal{M}$. In Fig. 2(a) we present the one-dimensional likelihood function normalized to its maximum value for $\otimes_Q$. There is a maximum at $\Omega_Q = 1$, in agreement with the analysis in [19]. In Fig. 3(a) we present the likelihood contours in the $\alpha - \beta$ parameter space, obtained after marginalizing over Ω_Q. Note that all values are allowed at the 2σ level. The confidence regions for the SnIa data correspond to quintessence models with $w_Q^0 < -0.4$ for $\Omega_Q = 0.6$, an upper limit that agrees with those found in [1,19].

B. Constraints from Doppler peaks and SnIa

We now compute the position of the three Doppler peaks l_1, l_2 and l_3 using Eq. (6). In addition to the parameter space used in the supernovae analysis we consider the physical baryon density and the scalar spectral index varying respectively in the range $\Omega_b h^2 \in (0.018, 0.026)$ and $n \in (0.9, 1.1)$. The Hubble constant is set to $h = 0.70$ in agreement with the recent HST observations [43]. The predicted peak multipoles in the CMB are then compared with those measured in the BOOMERANG and DASI spectra [18]. Note, that the third peak has been detected in the BOOMERANG data but not in the DASI data. Furthermore the authors of [18], with a model independent analysis, estimated the position of the peaks accurately at 1σ. However because the errors associated with the data are non-Gaussian, to be conservative we take our 1σ errors on the data to be larger than those reported in [18], so that our analysis is significant up to 2σ. We then evaluate a gaussian likelihood function $\mathcal{L}^{P]\dashv\|\int}(\alpha,\beta,\otimes_Q,\otimes_{\lfloor}\langle^{\epsilon},|)$. The combined one-dimensional likelihood function for the peaks is shown in Fig. 2(b), where we find $\Omega_Q = 0.69 \pm^{0.13}_{0.10}$. The likelihood for all the data sets combined is shown in Fig. 2(c), where we find $\Omega_Q = 0.75 \pm^{0.09}_{0.08}$. These results are in agreement with the analysis in [19,5,20].

The likelihood functions, combining all the data for the CMB peaks, for the scalar spectral index and the physical baryon density are shown in Fig. 4. Since the dependence of the peak multipoles on $\Omega_b h^2$ and n is small, it is not possible to obtain some significant constraints on these cosmological parameters using the location of the Doppler peaks. In Figs. 3(b)–3(d) we plot the two-dimensional likelihood function in

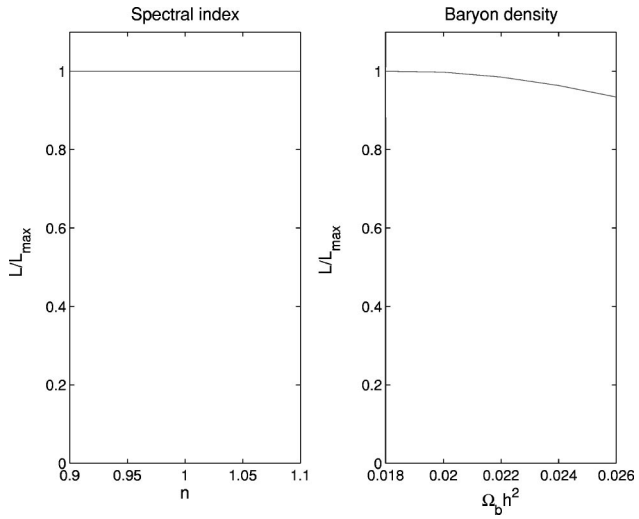

FIG. 4. One-dimensional likelihood for n and $\Omega_b h^2$.

the plane $\alpha-\beta$ for each peak, obtained after having marginalized over Ω_Q, $\Omega_b h^2$ and n. Their shape reflects the accuracy in the estimation of the position of the peaks. Actually the first one is very well resolved, while we are less confident with the location of the second and third peak. Therefore their likelihoods are more spread and flat in the $\alpha-\beta$ plane. The 1σ confidence contour [Fig. 3(b)] for the first acoustic peak constrains the slopes of our potential in the range: $3 \leqslant \alpha \leqslant 10$ and $1 \leqslant \beta \leqslant 3$. In particular the likelihood has a maximum at $\alpha=9$ and $\beta=2$, corresponding to an equation of state $w_Q^0=-0.8$ for $\Omega_Q=0.7$, in agreement with the recent analysis in [20]. However, the second and third peaks constrain a region where the equation of state is compatible with the cosmological constant value. Therefore the effect of including all the data (Fig. 5) in the likelihood analysis is to

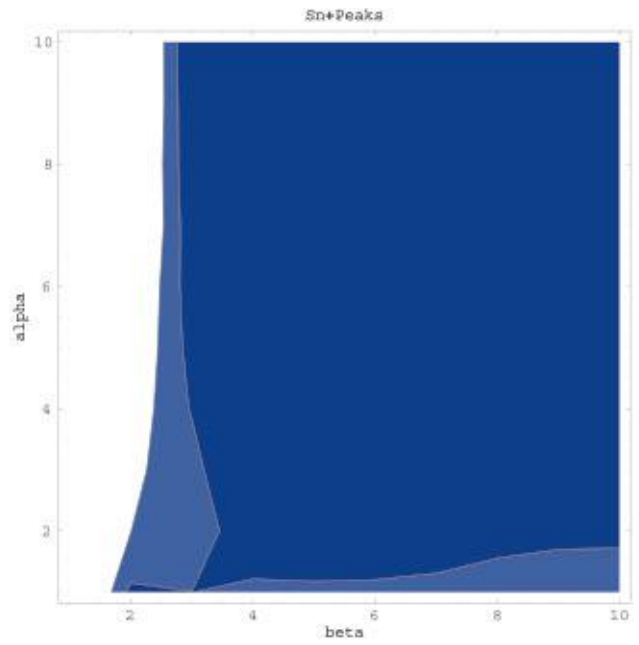

FIG. 5. (Color) Two-dimensional likelihood for SnIa and CMB with 1 (dark blue) and 2σ (light blue) contours.

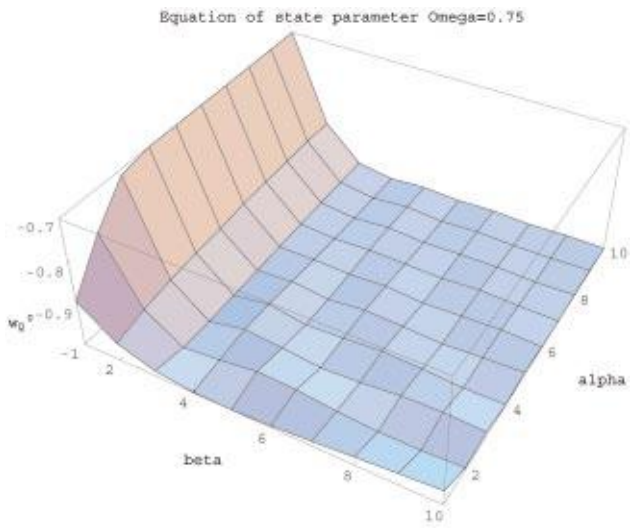

FIG. 6. (Color) Equation of state parameter against α and β for $\Omega_Q=0.75$. The 2σ contours correspond to models with $w_Q^0 \sim -1$.

move the constraint from models with $w_Q^0 \sim -0.8$ to models with an equation of state $w_Q^0 \sim -1$. As we can see in Fig. 6 the values of α and β, allowed by the likelihood including all the data (Fig. 5), correspond to our models with values of w_Q^0 in the range $-1 \leqslant w_Q^0 \leqslant 0.93$ at 2σ for our prior probability $\Omega_Q=0.75$. The reason for such a strong constraint is due to the assumed accurate determination of the third peak, in that it is insensitive to pre-recombination effects. In particular peak multipoles are shifted toward larger values as w_Q^0 approaches the cosmological constant value. This is because, in models with $w_Q^0 \sim -1$ the universe starts to accelerate earlier than in those with $w_Q^0 > -1$, consequently the distance to the last scattering surface is further and hence the sound horizon at the decoupling is projected onto smaller angular scales. Since the location of the third peak inferred in [18] is at $l_3=845\pm^{12}_{23}$, values of $w_Q^0 \sim -1$ fit this multipole better than models with $w_Q^0 > -1$. However we want to point out that at 1σ the position of the first peak is inconsistent with the position of the other two. A possible explanation of this discrepancy is that the multipoles l_2 and l_3 are less sensitive to small shift induced by the dependence on $\Omega_b h^2$ and n. Therefore we can obtain a different constraint on the dark energy equation of state if we consider the peaks individually.

V. CONCLUSIONS

The location of the sound horizon is very sensitive to the dark energy contribution. Due to the strong degeneracy in the shape of the CMB spectrum, a certain class of quintessence models can be better constrained using only the acoustic peaks. We have applied a likelihood analysis to constrain the shape of the quintessence potential, based on both the supernovae type Ia data and the positions of the CMB peaks. Assuming a flat space-time and making use only of the position of the first Doppler peak we find the best fit for models $w_Q^0 \sim -0.8$ for $\Omega_Q=0.7$ prior value. The combined analysis, including all three peaks and SnIa, gives the best fit for

$\Omega_Q = 0.75 \pm^{0.08}_{0.09}$. We have found in particular that the determination of third peak in the BOOMERANG data limits the equation of state parameter at 2σ in the range $-1 \leqslant w_Q^0 \leqslant -0.93$ for Ω_Q with this prior value. This has an important implication for minimally coupled quintessence models. Actually they must behave similarly to a cosmological constant, therefore inverse power law is disfavored. In fact, an equation of state parameter $w_Q^0 \sim -1$ implies the quintessence field is undergoing small damped oscillations around a minimum or evolving in a very flat region of the potential. For these reasons models like the double exponential potential [25] or the single modified exponential potential [35] pass this constraint, even though they are not included in our analysis. Another important caveat is that this study does not take into account quintessence scenarios where the contribution of the dark energy density in radiation or early in matter dominated eras is not negligible. In such a case we would have to take into account physical effects not only on distance measurements, but also on the structure formation process itself. These models and the non-minimally coupled ones therefore could yet be distinguished from a pure Λ CDM model. We still require a more complete analysis to understand the nature of the dark energy, but this paper points out that it is possible to constrain certain classes of models far more than was previously realized.

ACKNOWLEDGMENTS

We are very grateful to L. Amendola, A. Liddle, N. J. Nunes and J. Weller for useful discussions and comments.

[1] S. Perlmutter *et al.*, Astrophys. J. **517**, 565 (1999).
[2] A. Riess *et al.*, Astrophys. J. **117**, 707 (1999).
[3] P. De Bernardis *et al.*, Nature (London) **404**, 955 (2000).
[4] A. Balbi *et al.*, Astrophys. J. Lett. **545**, L1 (2000).
[5] C. B. Netterfield *et al.*, astro-ph/0104460.
[6] C. Pryke *et al.*, astro-ph/0104490.
[7] V. Sahni and A. Starobinsky, Int. J. Mod. Phys. D **9**, 377 (2000).
[8] R. R. Caldwell, R. Dave, and P. J. Steinhardt, Phys. Rev. Lett. **80**, 1582 (1998).
[9] I. Maor, R. Brustein, and P. J. Steinhardt, Phys. Rev. Lett. **87**, 049901 (2001).
[10] D. Huterer and M. S. Turner, Phys. Rev. D **64**, 123527 (2001).
[11] J. S. Alcaniz and J. A. S. Lima, Astrophys. J. Lett. **550**, L133 (2001).
[12] K. Benabed and F. Bernardeau, Phys. Rev. D **64**, 083501 (2001).
[13] A. Cappi, astro-ph/0105382.
[14] J. Weller and A. Albrecht, astro-ph/0106079.
[15] M. Kamionkowski and A. Buchalter, astro-ph/0001045.
[16] J. L. Crooks, J. O. Dunn, P. H. Frampton, and Y. J. Ng, astro-ph/0005406.
[17] M. Doran, M. Lilley, J. Schwindt, and C. Wetterich, astro-ph/0012139.
[18] P. De Bernardis *et al.*, astro-ph/0105296.
[19] G. Efstathiou, Mon. Not. R. Astron. Soc. **342**, 810 (2000).
[20] C. Baccigalupi, A. Balbi, S. Matarrese, F. Perrotta, and N. Vittorio, astro-ph/0109097.
[21] S. Perlmutter, M. Turner, and M. White, Phys. Rev. Lett. **83**, 670 (1999).
[22] L. Amendola, Phys. Rev. Lett. **86**, 196 (2001).
[23] A. Balbi, C. Baccigalupi, S. Matarrese, F. Perrotta, and N. Vittorio, Astrophys. J. Lett. **547**, L89 (2001).
[24] P. J. Steinhardt, L. Wang, and I. Zlatev, Phys. Rev. D **59**, 123504 (1999).
[25] T. Barreiro, E. J. Copeland, and N. J. Nunes, Phys. Rev. D **61**, 127301 (2000).
[26] A. Albrecht and C. Skordis, Phys. Rev. Lett. **84**, 2076 (1999).
[27] P. Brax and J. Martin, Phys. Lett. B **468**, 40 (1999).
[28] E. J. Copeland, N. J. Nunes, and F. Rosati, Phys. Rev. D **62**, 123503 (2000).
[29] B. Ratra and P. J. E. Peebles, Phys. Rev. D **37**, 3406 (1988).
[30] I. Zlatev, L. Wang, and P. J. Steinhardt, Phys. Rev. Lett. **82**, 896 (1999).
[31] P. G. Ferreira and M. Joyce, Phys. Rev. D **58**, 023503 (1998).
[32] A. Riazuelo and J. P. Uzan, Phys. Rev. D **62**, 083506 (2000).
[33] R. Bean, S. H. Hansen, and A. Melchiorri, astro-ph/0104162.
[34] W. Hu, N. Sugiyama, and J. Silk, Nature (London) **386**, 37 (1997).
[35] C. Skordis and A. Albrecht, astro-ph/0012195.
[36] L. Amendola, Phys. Rev. D **62**, 043511 (2000).
[37] F. Perrotta, C. Baccigalupi, and S. Matarrese, Phys. Rev. D **61**, 023507 (2000).
[38] C. Baccigalupi, S. Matarrese, and F. Perrotta, Phys. Rev. D **62**, 123510 (2000).
[39] P. Brax, J. Martin, and A. Riazuelo, Phys. Rev. D **62**, 103505 (2000).
[40] W. Hu, M. Fukugita, M. Zaldarriaga, and M. Tegmark, Astrophys. J. **549**, 669 (2001).
[41] M. Doran and M. Lilley, astro-ph/0104486.
[42] M. Doran, M. Lilley, and C. Wetterich, astro-ph/0105457.
[43] W. L. Freedman *et al.*, Astrophys. J. **553**, 47 (2001).